Dependence of Solids Conveying on Screw Axial Vibration in Single Screw Extruders

Qu Jinping, Shi Baoshan, Feng Yanhong, He Hezhi

The Key Laboratory of Polymer Processing Engineering, Ministry of Education, National Engineering Research Center of Novel Equipment for Polymer Processing, South China University of Technology, Guangzhou 510641, China

Received 27 September 2005; accepted 15 April 2006
DOI 10.1002/app.24658
Published online in Wiley InterScience (www.interscience.wiley.com).

ABSTRACT: In the single-screw extruder, the vibration force field is applied to the solids conveying process by the axial vibration of the screw and the novel concept on the solids conveying process being strengthened with the vibration force field has been brought forward in this study. We establish the mathematical model that describes the solids conveying process with the vibration force field and obtain the approximative analytical solutions of the pressure and velocity of the solids conveying in the down-channel. In the new theory, if the screw has no axial vibration the solids conveying pressure is the same as that of the Darnell and Mol theory, but the density and velocity of solids conveying along the screw channel is variable, which has modified the Darnell and Mol theory in which the density and velocity of the solids conveying along the screw channel was considered invariable. The results reveal that the axial vibration of the screw can increase the average pressure of solids conveying, decrease the channel length of the solids conveying section and increase the solids conveying angle.
 J Appl Polym Sci 102: 2998–3007, 2006

Key words: single screw extruder; vibration force field; solids conveying zone

INTRODUCTION

The single-screw extruder is the key equipment of plastic processing. Its performance is closely connected with screw geometry and operating conditions. The systematic investigation of the extrusion process has shown that no single mathematical model can be used to adequately describe the flow through the entire extruder in the literature.[1–4] That is, very different physical processes are controlling over different zones of the extruder. In other words, studies of the extrusion process are limited to the examination of one particular zone. Although the solids conveying zone is only a subsection of the extruder, it remains a major obstacle to the complete understanding and modeling of an extrusion process.

In comparison to the large of research on melt conveying in screw extruder, relatively little attention has been paid to the solid conveying for the complexity of the solid conveying process. But the solid conveying has important influence on the performance of the extruder. So, former researcher brought some theories forward by large hypothesis. In all classic work, Darnell and Mol were the first to obtain solutions for the solids conveying zone in screw extruders. More recently, there have been various refinements applied to their one-dimensional plug flow model by Schneider,[5] Tadmor and Broyer,[6,7] Lovegrove and Williams,[8–10] Chung,[2,11] and Zhu and Chen.[3,12–14] This classic work has provided a basis for many theoretical and experimental investigations of solids conveying zone. It is well-known that the model proposed by Darnell and Mol is in the form of plug flow. Then, the plug flow model suffers from several shortcomings. The most important one is that they do not predict the density variation, which actually exists in the extrusion process. Second, they assumed that the velocity of solids conveying along the screw channel is constant.

The gap between the practice and theory of extrusion is unreasonably large. In particular, the vibration force field is applied to the solids conveying process in the single-screw extruder.[15–18] It is our objective in this study to describe the novel concept on the solids conveying process being strengthened by the vibration force field and to discuss dependence of solids conveying on screw axial vibration in single screw extruders.

DESCRIPTION OF THE SOLIDS CONVEYING MODEL

The self-developed experimental extruder has not only natural characteristics, which the ordinary extruder has, but also the axial vibration of the screw. The sketch map of screw and barrel is shown in Figure 1. To simplify the solids conveying phenomenon and allow for an analytical solution, some assumptions are needed as follows.

Correspondence to: Q. Jinping (jpqu@scut.edu.cn).

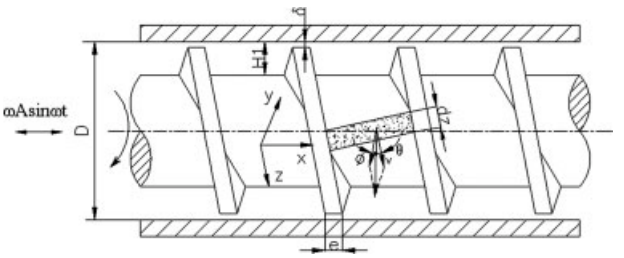

Figure 1 The sketch map of screw and barrel.

1. The moving solid polymer granules are compressible continuum in the channel;
2. The solid polymer granules are conveyed in the rectangle channel, which has the above moveable board, the two movable directions of the above moveable board and the material lie at an angle θ. It is shown in Figure 2;
3. The friction between the polymer and the wall of the channel only lies on the normal stress, and then it is independent of the velocity and the position of the material;
4. The angle is φ between the direction of the force that the moveable board acts on the polymer granules and the moving direction of the moveable board, and the change of the moving direction of the material is neglected, the average of the angle is $\bar{\varphi}$;
5. The ratio of the normal stress to the axial (the moveable direction) stress is constant (K), it is independent of the position, and the change of the stress distribution in the material is neglected;
6. The influence that the change of the material temperature brings is neglected;
7. The material density and the axial stress (tension) only change along the moving direction of the material;
8. Then, the solids conveying model based on the above assumptions can be gotten. It is shown in Figure 2.

MATHEMATICAL MODEL

A down-channel differential element is depicted in Figure 1. The continuity equation can be determined for the solid polymer granules by considering a conservation of mass of the differential element. Thus, the equation is:

$$\frac{\partial \rho}{\partial t} + v\frac{\partial \rho}{\partial z} + \rho\frac{\partial v}{\partial z} = 0 \tag{1}$$

where ρ is the material density at pressure p.

Experimental work of Chung[2] has indicated that the change of the material density can be expressed by an empirical equation of the form:

$$\rho = \rho_m - (\rho_m - \rho_a)\, e^{-C_0 p} \tag{2}$$

where ρ_m is the material density at the utmost pressure, ρ_a is the material density at the atmospheric pressure, p is pressure, C_0 is constant and is given according to experimental data.

Substituting eq. (2) into eq. (1) gives the expression

$$\frac{\partial p}{\partial t} + v\frac{\partial p}{\partial z} + \frac{1}{C_0}\left(\frac{\rho_m}{\rho_m - \rho_a}e^{C_0 p} - 1\right)\frac{\partial v}{\partial z} = 0 \tag{3}$$

Equation (3) is the continuity equation.

The equation of motion can be determined by applying a force and torque balance on a differential element of the solid polymer granules in the down-channel direction. The equation is given below.

$$\frac{\partial p}{\partial z} + K_f p + \rho\left(v\frac{\partial v}{\partial z} + \frac{\partial v}{\partial t}\right) = 0 \tag{4}$$

where

$$K_f = \frac{f_{w1}K}{H_1}\left[\frac{f_{w2}}{f_{w1}}\frac{W + 2H_1}{W} + f_{w2}\ \sin(\theta + \bar{\varphi}) - \cos(\theta + \bar{\varphi})\right] \tag{5}$$

To get the analytical solution of pressure and velocity in the channel, $\bar{p}$, $\bar{\rho}$, $\bar{v}$, t_0, ω_0, and L are defined as the dimensionless characteristic parameters of pressure, density, velocity, time, angular frequency, and length, respectively.

Assuming

$$\begin{cases} p = \bar{p}(1 + p^*) \quad \rho = \bar{\rho}(1 + \rho^*) \quad v = \bar{v}(1 + v^*) \\ A = LA^* \quad t = t_0 t^* \quad \omega = \omega_0 w^* \quad z = Lz^* \end{cases} \tag{6}$$

By substituting eq. (6) into eq. (3) and considering $\bar{v}t_0/L \ll 1$, $v^* \le 1$, $e^{C_0\bar{p}p^*} - 1 \ll 1$, the dimensionless expression of the continuity equation is shown as

$$\frac{\partial p^*}{\partial t^*} + \frac{1}{S_h}\frac{\partial p^*}{\partial z^*} + \frac{B_h}{S_h}\frac{\partial v^*}{\partial z^*} = 0 \tag{7}$$

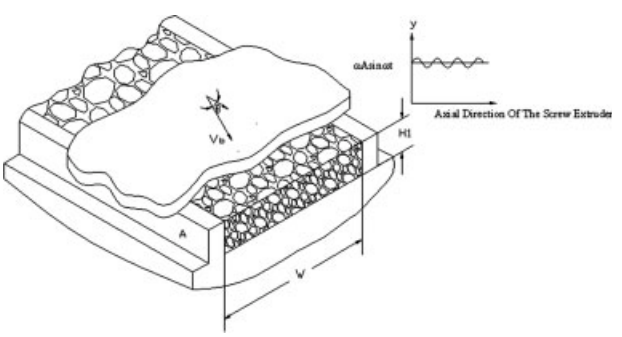

Figure 2 Schematic diagram of solid conveying model.

where

$$S_h = \frac{L}{\bar{v}t_0} \tag{8}$$

$$B_h = \frac{\bar{\rho}e^{C_0\bar{p}}}{C_0\bar{p}(\rho_m - \rho_a)} \tag{9}$$

By substituting eq. (6) into eq. (4) and considering $v^* \le 1,\ \rho_m\bar{v}^2/\bar{p} \ll 1$, the dimensionless expression of the equation of motion is shown as

$$\frac{\partial p^*}{\partial z^*} + C_h p^* + D_h\frac{\partial v^*}{\partial z^*} + E_h\frac{\partial v^*}{\partial t^*} + C_h = 0 \tag{10}$$

where

$$C_h = LK_f \tag{11}$$

$$D_h = \frac{\rho_m\bar{v}^2}{\bar{p}} \tag{12}$$

$$E_h = D_hS_h = \frac{\rho_m\bar{v}L}{t_0\bar{p}} \tag{13}$$

APPROXIMATE ANALYTICAL SOLUTION

To analyze the continuity equation and the equation of motion, omitting the superscripts in the eqs. (7) and (10), a differential equation group is given below. An amendatory coefficient (k) must be added into the equation group for difference that is introduced by linearizing the equations.

$$\begin{cases} \dfrac{\partial p}{\partial t} + \dfrac{k}{S_h}\dfrac{\partial p}{\partial z} + \dfrac{B_h}{S_h}\dfrac{\partial v}{\partial z} = 0 \\ \dfrac{\partial p}{\partial z} + C_h p + kD_h\dfrac{\partial v}{\partial z} + E_h\dfrac{\partial v}{\partial z} + C_h = 0 \end{cases} \tag{14}$$

In the case, the dimensionless initial conditions is $v(z,t)|_{t=0} = 0,\ p(z,t)|_{t=0} = 0$. Transforming eq. (14) by Laplace expansion obtains

$$\begin{cases} sP(s) + \dfrac{k}{S_h}\dfrac{\mathrm{d}P(s)}{dz} + \dfrac{B_h}{S_h}\dfrac{\mathrm{d}V(s)}{dz} = 0 \\ \dfrac{\mathrm{d}P(s)}{\mathrm{d}z} + C_hP(s) + kD_h\dfrac{\mathrm{d}V(s)}{\mathrm{d}z} + sE_hV(s) + \dfrac{1}{s}c_h = 0 \end{cases} \tag{15}$$

With the aid of eq. (15), a two-order differential equation group is obtained

$$\begin{cases} \dfrac{\mathrm{d}^2P(s)}{\mathrm{d}z^2} + \beta\dfrac{\mathrm{d}P(s)}{\mathrm{d}z} - \lambda^2P(s) = 0 \\ \dfrac{\mathrm{d}^2V(s)}{\mathrm{d}z^2} + \beta\dfrac{\mathrm{d}V(s)}{\mathrm{d}z} - \lambda^2V(s) = \dfrac{S_hC_h}{B_h - K^2D_h} \end{cases} \tag{16}$$

where

$$\beta = \frac{B_hC_h - sk(S_hD_h + E_h)}{B_h - k^2D_h} = \beta_1 - s\beta_2 \tag{17}$$

$$\lambda^2 = \frac{S_hE_h}{B_h - k^2D_h}s^2 = bs^2 \tag{18}$$

In the case, eq. (16) should meet the following boundary conditions.

$$\begin{cases} p(z,t)|_{z=0} = p_0(t) \\ v(z,t)|_{z=0} = v_0(t) \end{cases} \tag{19}$$

then, transforming eq. (19) by Laplace expansion obtains

$$\begin{cases} P(s)|_{z=0} = L[p_0(t)] = P_0(s) \\ V(s)|_{z=0} = L[v_0(t)] = V_0(s) \end{cases} \tag{20}$$

Solving eq. (16) obtains

$$\begin{cases} P(s) = \dfrac{sE_h}{a_1 - a_2}(e^{r_1z} - e^{r_2z})V_0(s) + \dfrac{C_h}{(a_1 - a_2)s}(e^{r_1z} - e^{r_2z}) \\ \qquad - \dfrac{1}{a_1 - a_2}\cdot(a_2e^{r_1z} - a_1e^{r_2z})P_o(s) \\ V(s) = \dfrac{1}{sE_h(a_1 - a_2)}\left[sE_h(a_1e^{r_1z} - a_2e^{r_2z})V_0(s) - \dfrac{C_h}{s^2E_h}\right. \\ \qquad \left. - a_1a_2(e^{r_1z} - e^{r_2z})P_0(s) + \dfrac{C_h}{s}(a_1e^{r_1z} - a_2e^{r_2z})\right] \end{cases} \tag{21}$$

where

$$r_1 = \frac{-\beta + \sqrt{\beta^2 + 4\lambda^2}}{2} \tag{22}$$

$$r_2 = \frac{-\beta - \sqrt{\beta^2 + 4\lambda^2}}{2} \tag{23}$$

$$a_1 = \frac{kD_h}{B_h}(sS_h + kr_1) - r_1 - C_h \tag{24}$$

$$a_2 = \frac{kD_h}{B_h}(sS_h + kr_2) - r_2 - C_h \tag{25}$$

If $v_0(t)$ is the power of system, the steady response of the first term value of eq. (21) can be gotten when the power of system is the exponent function of imaginary number, in other words, if $v_0(t) = v_me^{j\omega t}$, then

$$p_1(z,t) = \frac{sE_h}{a_1 - a_2}(e^{r_1 z} - e^{r_2 z})\big|_{s=jw}\ v_m e^{j\omega t} \tag{26}$$

If

$$v_0(t) = v_m I_m e^{j\omega t} = v_m\ \sin\omega t \tag{27}$$

where

$$v_m = \frac{\omega A\ \sin\theta}{\bar{v}} \tag{28}$$

Then, the Laplacian (s) is tending to zero when time is infinite according to terminal value theorem and $\beta_2 \ll 1$ the result of the eqs. (26) and (27) are given respectively, as

$$p_1(z,t) = \frac{2v_m\omega B_h E_h}{(k^2 D_h - B_h)\alpha} e^{-\beta_1/2z}\ sh\left(\frac{1}{2}\alpha z\right)\ \cos\omega t \tag{29}$$

$$v_1(z,t) = \frac{-v_m\beta_1}{\alpha} e^{-\beta_1/2z}\ sh\left(\frac{1}{2}\alpha z\right)\ \sin(\omega t + \varphi') \sqrt{\left[1 + \frac{\alpha}{\beta_1} cth\left(\frac{\alpha z}{2}\right)\right]^2 + \left(\frac{2E_h\omega}{B_h C_h}\right)^2} \tag{30}$$

where

$$\alpha = \sqrt{\beta_1^2 - 4b\omega^2} \tag{31}$$

$$\varphi' = tg^{-1}\left\{-2E_h\omega \Big/ B_h C_h\left[1 + \frac{\alpha}{\beta_1} cth\left(\frac{\alpha z}{2}\right)\right]\right\} \tag{32}$$

The steady responses of the other term values of eq. (21) can be gotten by the terminal value theorem.

$$p_2(z,t) = \lim_{s\to 0} \frac{sB_h}{(k^2 D_h - B_h)\alpha}(a_2 e^{r_1 z} - a_1 e^{r_2 z})\frac{p_0}{s} = -p_0 e^{-\beta_1 z} \tag{33}$$

$$p_3(z,t) = \lim_{s\to 0} \frac{sC_h B_h}{(k^2 D_h - B_h)\alpha s}(e^{r_1 z} - e^{r_2 z}) = e^{-\beta_1 z} - 1 \tag{34}$$

$$v_2(z,t) = \lim_{s\to 0} s\frac{B_h a_1 a_2}{sE_h(k^2 D_h - B_h)\alpha}(e^{r_1 z} - e^{r_2 z})\frac{p_0}{s} = \frac{p_0}{E_h}(1 - e^{-\beta_1 z})\frac{D_h S_h}{B_h} = \frac{1}{B_h} p_0 (1 - e^{-\beta_1 z}) \tag{35}$$

$$v_3(z,t) = \lim_{s\to 0} s\left[\frac{C_h B_h}{s^2 E_h(k^2 D_h - B_h)\alpha}\ (a_1 e^{r_1 z} - a_2 e^{r_2 z}) - \frac{C_h}{s^2 E_h}\right] = \lim_{s\to 0}\left(\frac{C_h}{sE_h} - \frac{C_h}{sE_h}\right) = 0 \tag{36}$$

then

$$\begin{cases} p(z,t) = \dfrac{2v_m\omega B_h E_h}{(k^2 D_h - B_h)\alpha} e^{-\beta_1/2z}\ sh\left(\dfrac{1}{2}\alpha z\right)\ \cos\omega t + (1 + p_0)e^{-\beta_1 z} - 1 \\ v(z,t) = \dfrac{v_m\beta_1}{\alpha} e^{-\beta_1/r2z}\ sh\left(\dfrac{\alpha z}{2}\right)\ \sin(\omega t + \varphi)\sqrt{\left[1 + \dfrac{\alpha}{\beta_1} cth\left(\dfrac{\alpha z}{2}\right)\right]^2 + \left(\dfrac{2E_h\omega}{B_h C_h}\right)^2}\ +\ \dfrac{p_0}{B_h}(e^{-\beta_1 z} - 1) \end{cases} \tag{37}$$

where

$$\beta_1 = \frac{K_f L\rho_a}{\rho_0 - k^2\rho_m C_0 v_0^2(\rho_m - \rho_a)} \tag{38}$$

$$b = \frac{\rho_m(\rho_m - \bar{\rho})C_0 L^2}{[\bar{\rho} - k^2\rho_m(\rho_m - \bar{\rho})C_0 v_0^2]t_0^2} \tag{39}$$

$$E_h = \frac{\rho_m \bar{v} L}{\bar{p} t_0} \tag{40}$$

$$B_h = \frac{\bar{\rho} e^{C_0\bar{p}}}{C_0\bar{p}(\rho_m - \rho_a)} = \frac{\bar{\rho}}{(\rho_m - \bar{\rho})C_0\bar{p}} \tag{41}$$

If the average of the down-channel direction (z direction is considered as the dimensionless characteristic parameters of pressure ($\bar{p}$) when the amplitude of the axial vibration of the screw is zero, in other words,

$$\bar{p} = \frac{1}{Z_1}\int_0^z p_0 e^{\beta_1/Lz} dz \tag{42}$$

where Z_1 is the length of the channel in the down-channel direction. Then, according to eqs. (2) and (42), the dimensionless characteristic parameters of density is

$$\bar{\rho} = \rho_m - (\rho_m - \rho_a)\ e^{-C_0\bar{p}} \tag{43}$$

If the velocity of the material at the inlet of the channel is $v_0(t) = v_0(1 + A\ \sin\omega t)$, to ensure the dimensionless term $v_0(t)$ is pulsating power, in other words, if $v_0(t) = v_m\ \sin\omega t$, then

$$\bar{v} = v_0 \tag{44}$$

Equation (37) is approximate analytical solutions of the pressure and velocity in the down-channel when the vibration force field is applied to the solids conveying process.

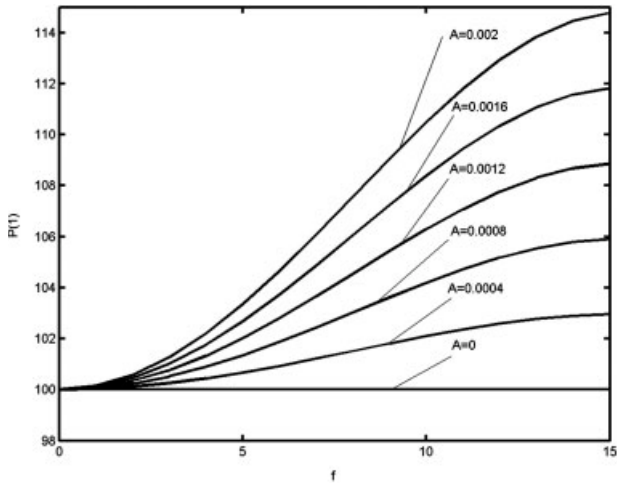

Figure 3 Influence of the amplitude and frequency of the vibration on the dimensionless pressure of the channel.

RESULTS AND DISCUSSION

Pressure distribution

As we known from the above approximate analytical solution that the pressure and velocity of the channel are cyclical variation. In fact, the compressed material is elastic-plastic body. The material can be compressed into a certain state with the instantaneous pressure is up to the maximum in one vibration period, the material have elastic deformation and plastic deformation, so the compressed material have back-moving distance, which is less than the compressed distance, with the instantaneous pressure fall to the minimum in the vibration period. For the material density, it can be considered that the instantaneous pressure is equivalent to a virtual value of the certain pressure. The standard deviations of the instantaneous pressure can be considered as the virtual value of the certain pressure.

$$p_{1e}(z) = \sqrt{\frac{1}{t_0}\int_0^{t_0} p_1^2(z)\ \cos^2 \omega t dt} = \frac{1}{\sqrt{2}}|p_{1m}(z)| \quad (45)$$

where $p_{1m}(z)$ is the amplitude function of eq. (29)

$$|p_{1m}(z)| = \frac{2v_m \omega b B_h}{S_h \alpha} e^{-\beta_1/2z} sh\left(\frac{1}{2}\alpha z\right) \quad (46)$$

then

$$p_e(z) = \frac{1}{\sqrt{2}}|p_{1m}(z)| + (1+p_0)e^{-\beta_1 z} - 1 \quad (47)$$

Letting $z = 1$, $p_0(1) = 100$, $\beta_1 = -1.1$, $b = 0.00223$, Figure 3 can be drawn according to eq. (47). It shows that the dimensionless pressure of the channel increases with the increases of amplitude and frequency of the vibration when the dimensionless length of the channel is 1.

Rewriting eq. (47) with dimension:

$$p_e(z) = \frac{\bar{p}}{\sqrt{2}}|p_{1m}(z)| + p_0 e^{-\beta_1/Lz} \quad (48)$$

If the screw has no axial vibration, eq. (48) reduces to

$$p_e(z) = p_0 e^{-\beta_1/Lz} \quad (49)$$

Then, when the amplitude of the vibration is zero or not, the relative degree of the material compressed density can be defined as

$$\xi_p = \frac{\rho(z) - \rho_s}{\rho_s} = \frac{(\rho_m - \rho_a)(e^{-C_0 p_t} - e^{-C_0 p_t(z)})}{\rho_m - (\rho_m - \rho_a)e^{-C_0 p_t}} = \frac{(\rho_m - \rho_a)e^{-C_0 p_s}(1 - e^{C_0 \bar{p}/\sqrt{2}p_{1m}})}{\rho_m - (\rho_m - \rho_a)e^{-C_0 p_s}} \quad (50)$$

Considering $4b\omega^2/\beta_1^2 = 1$, eq. (47) reduce to

$$p_e(z) \approx \frac{v_m \omega b B_h}{\sqrt{2} S_h \beta_1}(1 - e^{-\beta_1 z}) + (1 + p_0)e^{-\beta_1 z} - 1 \quad (51)$$

Letting $p_0(0) = 100$, $\beta_1 = -1.1$, $b = 0.002$, $1 + p_0 = 0.035$, $L\omega\ bB/\sqrt{2}S\beta_1 \bar{v} \sin\theta = 0.92$, Figures 4–6 can be drawn according to eq. (51). Figure 4 shows the diagram is same to Figure 3 within the range of practical operating conditions when the dimensionless length of the channel is 1. Figure 5 shows the effect of the frequency on the dimensionless pressure of the channel can be drawn the when amplitude of the vibration is constant ($A = 0.001$). Figure 6 shows the effect of the amplitude on the dimensionless pressure of the channel can be drawn when frequency of the vibration is constant ($\omega = 1$).

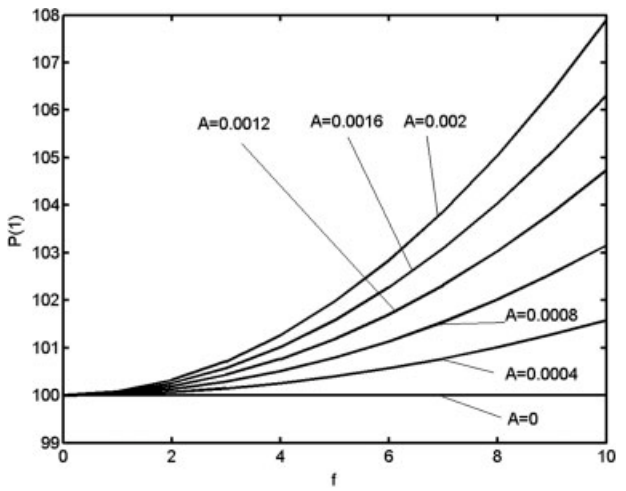

Figure 4 Influence of the amplitude and frequency of the vibration on the dimensionless pressure of the channel.

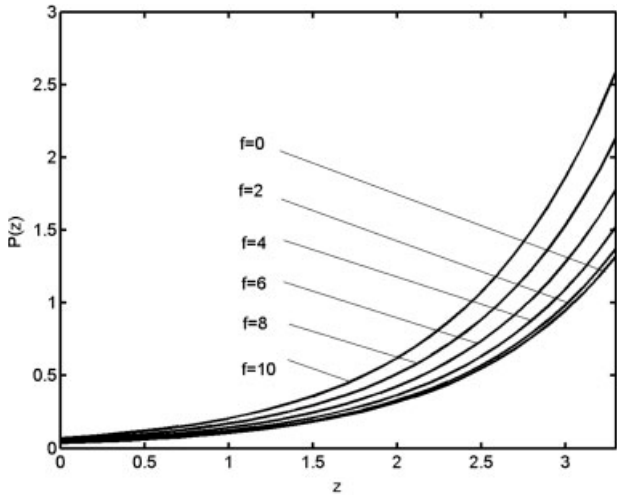

Figure 5 Effect of the frequency on the dimensionless pressure of the channel.

From the above four figures, a conclusion can be got that the pressure built up with vibration is higher than the pressure built up without vibration on the same spot of the channel; the vibration frequency and the amplitude have a significant influence on the degree of the build-up pressure. The pressure increases with the increase of frequency and amplitude.

Rewriting eq. (51) with dimension:

$$p_e(z) \approx \frac{\rho_m \sin\theta}{\sqrt{2}|K_f|}(e^{-\beta_1 z/L} - 1)A\omega^2 + p_0 e^{-\beta_1 z/L} \qquad (52)$$

To express influence of the vibration on the dimensionless pressure of the channel definitely the relative degree of the build-up pressure can be defined as the impact factor (ε_p), which the vibration acts on the pressure when the amplitude of the vibration is zero or not.

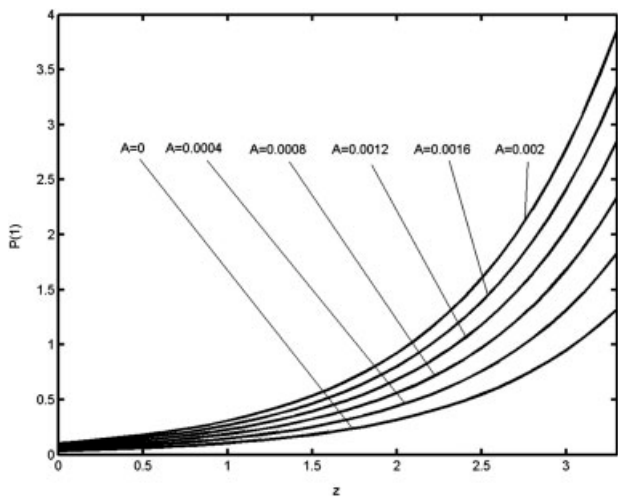

Figure 6 Effect of the amplitude on the dimensionless pressure of the channel.

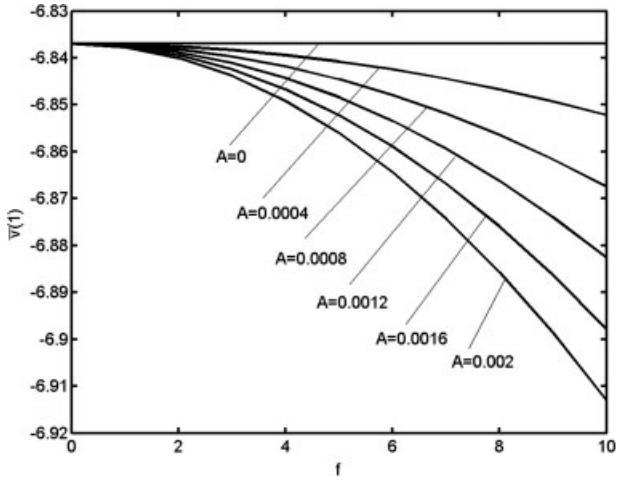

Figure 7 Influence of the amplitude and frequency of the vibration on the dimensionless velocity of the solid polymer granules.

$$\xi_p = \frac{p_e(z) - p_s(z)}{p_s(z)} = \frac{\rho_m \sin\theta}{\sqrt{2}p_0|K_f|}\left(1 - e^{-\beta_1 z/L}\right)A\omega^2 \qquad (53)$$

According to the front analysis, β_1 less than zero, then from eq. 53, we can get the impact factor (ξ_p) increases with the increases of amplitude and frequency of the vibration.

Velocity distribution

Velocity can be analyzed by the same way with the pressure, and then velocity also has a virtual value. For $4b\omega^2/\beta_1^2 \ll 1$, $(2E_h\omega/B_hC_h)^2\,(e^{-\beta_1^2}-1)^2 \ll 1$, the expression is obtained from eq. (37)

$$v_e(z) = \left(\frac{p_0}{B_h} - \frac{\sqrt{2}L\omega_0 E_h \sin\theta}{\bar{v}B_h|C_h|}A\omega^2\right)\left(e^{-\beta_1 z} - 1\right) \qquad (54)$$

Letting $v(0) = -6.84$, $\beta = -1.1$, $\sqrt{2}EL\omega \sin\theta/B.C.\bar{V} = 3.4$, $p_0/B = -0.19$, the following figures can be drawn according to eq. (54). Figure 7 shows that the dimensionless velocity of the solid polymer granules in the channel decreases with the increases of the amplitude and frequency of vibration when the dimensionless length of the channel is 1. When amplitude of the vibration is constant ($A = 0.01$), effect of the frequency of vibration on the dimensionless velocity of the solid polymer granules can be drawn in the Figure 8. When frequency of the vibration is constant ($\omega = 1$), effect of the amplitude of vibration on the dimensionless velocity of the solid polymer granules can be drawn in the Figure 9.

The above three figures show that the velocity of the solids conveying in the channel decreases with power-law is contrary to the pressure that increases with power-law; the dimensionless velocity of the solid

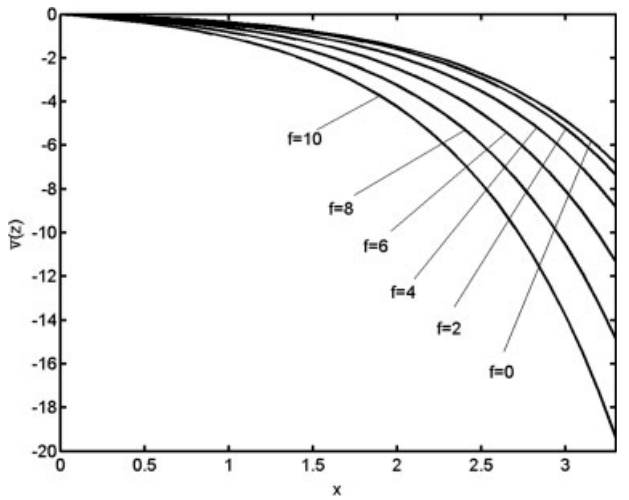

Figure 8 Influence of the frequency of vibration on the dimensionless velocity of the solid polymer granules.

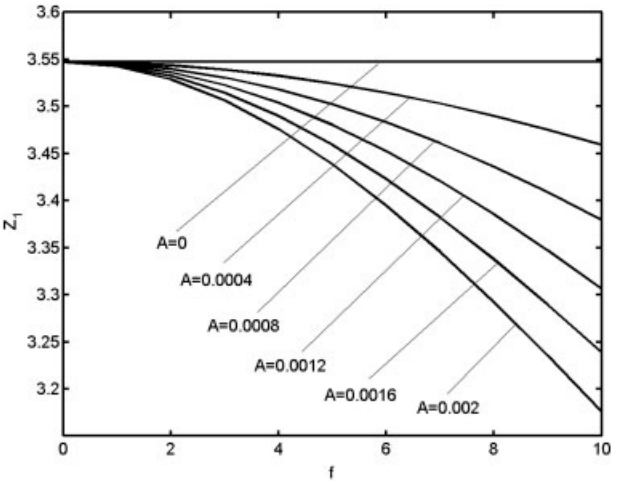

Figure 10 Influence of the amplitude and frequency of the vibration on the length of the solids conveying zone.

polymer granules in the channel decreases with the increases of the amplitude and frequency of vibration. The reason is that pressure increases with the increases of amplitude and frequency of the vibration at certain position. With the increase of pressure, potential energy of the pressure and elastic potential energy of the differential element are raised; the energy of motion about the differential element is decreased according to conservation of energy principle, then the velocity of the differential element decreased.

Rewriting eq. (54) with dimension:

$$v_e(z) = \frac{\sqrt{2}\rho_m(\rho_m - \bar{\rho})C_0 v_0}{\bar{\rho}K_f} \sin\theta(e^{-\beta_1\frac{z}{L}} - 1)A\omega^2 + v_0\left[1 - \frac{C_0(\rho_m - \bar{\rho})(\bar{p} - p_0)}{\bar{\rho}}\left(e^{-\beta_1\frac{z}{L}} - 1\right)\right] \quad (55)$$

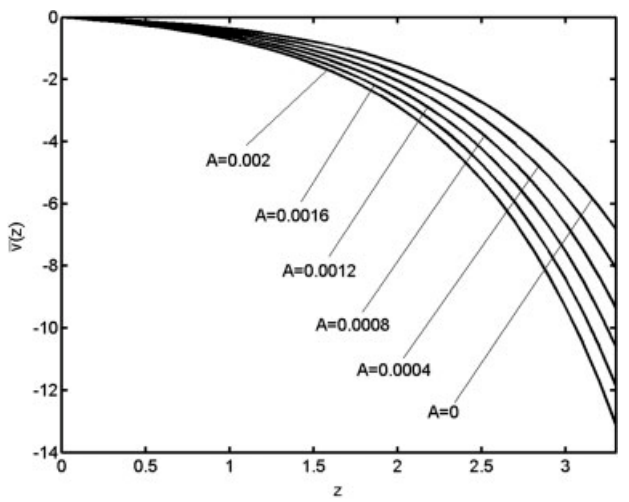

Figure 9 Influence of the amplitude of vibration on the dimensionless velocity of the solid polymer granules.

When v_m is zero, it is no vibration, then eq. (55) reduces to

$$v_s(z) = v_0\frac{C_0 v_0(\rho_m - \bar{\rho})(\bar{p} - p_0)}{\bar{\rho}}(e^{-\beta_1\frac{z}{L}} - 1) \quad (56)$$

Length of the solids conveying zone

According to eq. (49), the length of the solids conveying zone without vibration force field can be given as

$$Z_1 = \frac{1}{\beta_1}\ln\frac{1 + p_0}{1 + p_s(z)} \quad (57)$$

According to eq. (51), the length of the solids conveying zone with vibration force field can be given as

$$Z_1 = \frac{1}{\beta_1}\ln\frac{1 + p_0 - \frac{v_m\omega b B_h}{\sqrt{2}S_h\beta_1}}{1 + p_e(z) - \frac{v_m\omega b B_h}{\sqrt{2}S_h\beta_1}} \quad (58)$$

When the build-up pressure is a certain value, it means the solids conveying zone is the end. Letting $p_e(z) = 5$, $\beta_1 = -1.1$, $b = 0.002$, $p_a = 0.1$, $\frac{L\omega_0 b B_h}{\sqrt{2}s_h\beta_1} = 0.09$ in eq. (51), Figure 10 can be drawn. It shows that the dimensionless length of the solids conveying zone decreases with the increases of the amplitude and frequency of the vibration. From the figure, a conclusion can be got that the length of the solids conveying zone is shorter when the vibration force field is applied to the solids conveying process; the needful length decreases with the increase of frequency and amplitude.

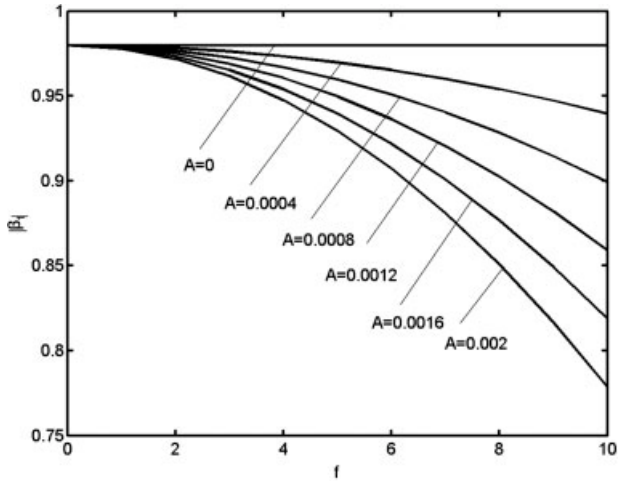

Figure 11 Influence of the amplitude and frequency of the vibration on the conveying angle of the solid.

Conveying angle of the solid

Now the influence of the vibration on the conveying angle will be discussed. For $4b\omega^2/\beta_1^2 = 1$, eq. (52) can be rearranged as

$$\frac{v_m\omega bt_0B_h\bar{p} + \sqrt{2}S_h|\beta_1|p_0}{v_m\omega bt_0B_h\bar{p} + \sqrt{2}S_h|\beta_1|p_e(z)}e^{-\frac{\beta_1}{L}z} = 1 \tag{59}$$

Solving eq. (59), obtains

$$|\beta_1| \approx 1 - \frac{p_0}{p_e(L)} - \frac{B_hv_m\omega bt_0}{\sqrt{2}S_h}\frac{\bar{p}}{p_e(L)} = 1 - \frac{p_0}{p_e(L)}\left(1 + \frac{B_hv_m\omega bt_0}{\sqrt{2}S_h}\frac{\bar{p}}{p_0}\right) \tag{60}$$

If $\bar{p} = p_e(L)$, eq. (60) reduces to

$$|\beta_1| = 1 - \frac{p_0}{p_e(L)} - K_\beta A\omega^2 \tag{61}$$

where

$$K_\beta = \frac{B_h\omega_0 bt_0\ \sin\theta}{\sqrt{2}S_h\bar{v}} \tag{62}$$

therefore

$$|K_f| \approx \frac{|\beta_1|}{L} = \frac{1}{L} - \frac{p_0}{Lp_e(L)} - K_\beta A\omega^2 \tag{63}$$

According to eq. (5) obtains

$$\bar{\varphi} = \arcsin\left[\frac{1}{f_{w1}\sqrt{1^2+f_{w2}^2}}\left(\frac{H_1K_f}{K} - \frac{f_{w2}(W+2H_1)}{W}\right)\right] + \phi_1 - \theta \tag{64}$$

where

$$\phi_1 = \arctan\frac{1}{f_{w2}} \tag{65}$$

Letting $p_e(L) = 50$, $p_0 = 1.01$, $k_\beta = 5\times10^{-5}$ in eq. (61), influence of the amplitude and frequency of the vibration on $|\beta_1|$ can be shown by Figure 11. The figure shows that $|\beta_1|$ decrease with the increase of the amplitude and frequency of the vibration. $|K_f|$ is linearly proportional to $|\beta_1|$ according to eq. (63); from eq. (64), the conveying angle of the solid increases with $|K_f|$ decreases. Thus, it is useful to increase the conveying angle of the solid that the vibration force field is applied to the solids conveying process.

EXPERIMENTAL

Equipment and material

The self-developed experimental extruder has half-opened barrel. The geometric parameters of the extruder are given in Table I.

The material used in this experiment is low-density polyethylene (LDPE), and its physical characteristics are shown in Table II.

Method

To differentiate solid from melt, little black carbon is added to the granule of LDPE (Fig. 12). The experimental parameters are as follows:

1. The speed of the screw is adjustable at the 60 rpm;
2. The range of vibration frequencies of the screw in the axial direction is 5–25 Hz;
3. The range of vibration amplitudes of the screw in the axial direction is 0–0.25 mm;
4. The temperature is constant, and it is set as 140°C.

TABLE I
Geometric Parameters of the Solids Conveying Section of the Screw

Diameter of screw	Length of the solids conveying zone	Helix angle of screw	Depth of helix channel	Width of helix channel	Width of helix flight
20 mm	120 mm	17.65°	3.2 mm	17 mm	2 mm

TABLE II
Physical Characteristics of the Material Used in the Experiment

Material	ρ_m (g/cm^3)	ρ_a (g/cm^3)
LDPE	0.92	0.52

According to the abovementioned parameters, the experiment is carried out as follows:

Keeping the vibration frequency constant and varying the vibration amplitude;
Keeping the vibration amplitude constant and varying the vibration frequency.

Result

The curves shown in Figures 13 and 14 present the experimental results; the results show that the measured pressure on the endpoint of solid conveying with vibration is higher than the pressure without vibration and the measured pressure goes up with nonlinear rule. In Figures 13 and 14, comparing all curves, the same trend derived from these curves. It is that the measured pressure increases with the increases of the frequency or amplitude.

Figure 15 shows the curves of the distance between end points of solid conveying with vibration and the end point without vibration when varying amplitude with fixed frequency. The curves illustrate an important point. The endpoint of solid conveying with vibration is nearer the inlet of the material than the endpoint without vibration, and the distance between the endpoint of solid conveying and the inlet of the material is shortening with increasing amplitude or frequency. Comparing Figure 15 with Figure 13, an important point is got. These curves accord with a rule that the shorter length of solid conveying relative to the higher pressure.

Figure 12 Photo of sampling. [Color figure can be viewed in the online issue, which is available at www.interscience.wiley.com.]

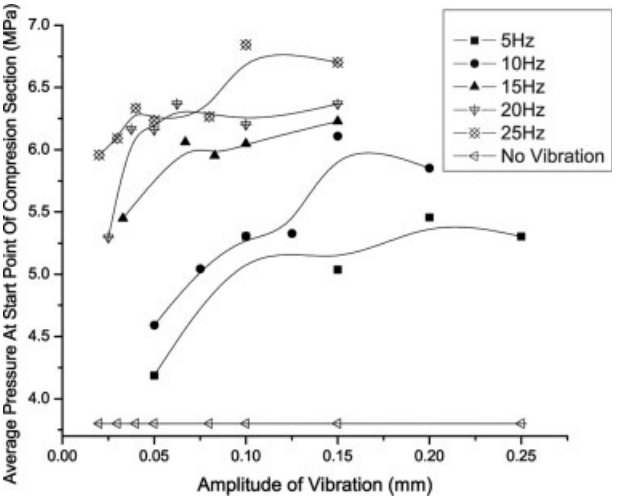

Figure 13 Relationship between the average pressure and amplitude.

CONCLUSIONS

By analyzing the abovementioned results, some conclusions can be drawn as follows:

1. The build-up pressure of the channel increases with the increases of the amplitude and frequency of the vibration.
2. The conveying angle of the solid increases with the increases of the amplitude and frequency of the vibration.

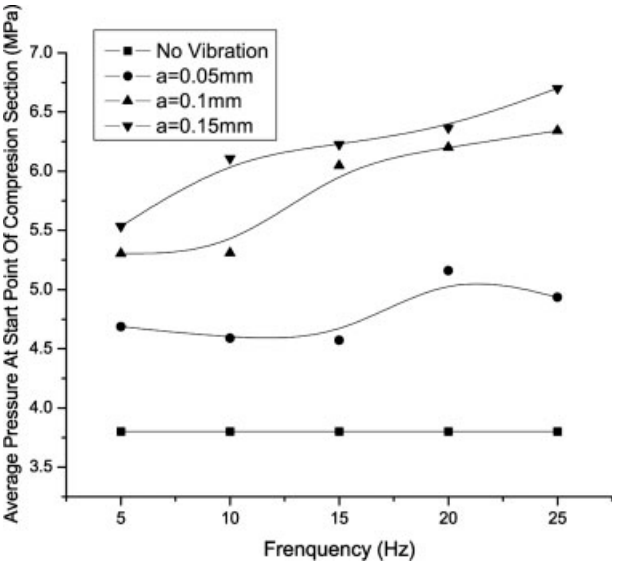

Figure 14 Relationship between the average pressure and frequency.

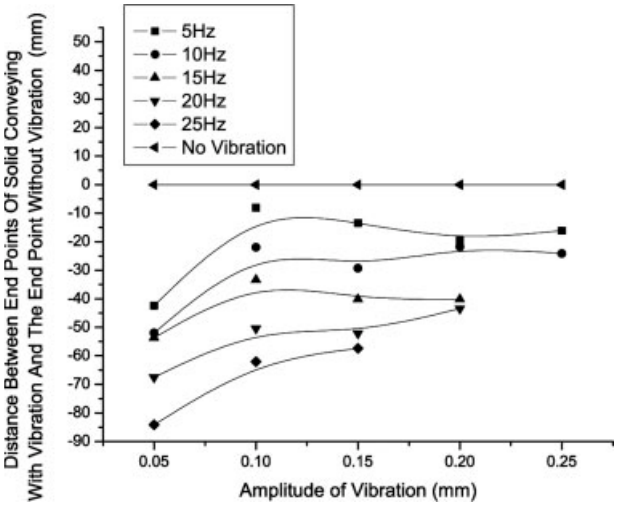

Figure 15 Curves of the distance between end points of solid conveying with vibration and the end point without vibration when varying amplitude with fixed frequency.

3. The axial vibration of the screw can decrease the channel length of the solids conveying section.

All these are novel concepts and new theory of solids conveying in single screw extruders when the vibration force field is applied to the solids conveying process. In contrast to the classical theory of solids conveying, the gap between the practice and theory of extrusion is smaller. The conclusions are useful to predict the overall performance of a screw extruder when the vibration force field is applied to the extrusion process.

NOMENCLATURE

A amplitude
C_0 constant
f frequency
f_{w1} coefficient of friction between the barrel and solid polymer granules
f_{w1} coefficient of friction between the channel and solid polymer granules
H_1 depth of channel
K the ratio of the normal stress to the axile stress
L length of the solids conveying zone
p pressure
$\bar{p}$ dimensionless characteristic parameters of pressure
p_e equivalent pressure
p_s steady pressure
p_0 initial pressure
t time
t_0 dimensionless characteristic parameters of time
v velocity
$\bar{v}$ dimensionless characteristic parameters of velocity
v_e equivalent velocity
v_s steady velocity
v_0 initial velocity
W width of channel
φ angle between the direction of the force that the moveable board acts on the polymer granules and the moving direction of the moveable board
$\bar{\varphi}$ average of the angle φ
γ amendatory coefficient
θ angle between the moveable directions of the above moveable board and the material
ρ density
$\bar{\rho}$ dimensionless characteristic parameters of density
ρ_m the material density in the utmost pressure
ρ_a the material density in the atmospheric pressure
ω angular frequency

References

1. Darnell, W. H.; Mol, E. A. J. Polym Eng Sci 1956, 12, 20.
2. Chung, C. I. SPE J 1970, 26, 32.
3. Zhu, F.; Chen, L. Polym Eng Sci 1991, 31, 1113.
4. Hyun, K. S.; Spalding, M. A.; Hinton, C. E. J Reinf Plast Compos 1997, 16, 1211.
5. Schneider, K. Technical Report on Plastics Processing Processes in the Feeding Zone of an Extruder, Institute of Plastics Processing (IKV), Aachen, 1969.
6. Broyer, E.; Tadmor, Z. Polym Eng Sci 1972, 12, 12.
7. Tadmor, Z.; Broyer, E. Polym Eng Sci 1972, 12, 378.
8. Lovegrove, J. G. A.; Williams, J. G. J Mech Eng Sci 1973, 15, 114.
9. Lovegrove, J. G. A.; Williams, J. G. J Mech Eng Sci 1973, 15, 195.
10. Lovegrove, J. G. A.; Williams, J. G. Polym Eng Sci 1974, 14, 589.
11. Chung, C. I. Polym Eng Sci 1975, 15, 29.
12. Fuhua, Z. Polym Mater Sci Eng 1986, 3, 1.
13. Fuhua, Z.; Shizeng, F. Polym Mater Sci Eng 1987, 4, 22.
14. Shunliang, J.; Fuhua, Z. China Plast Ind, 1997, 2, P83.
15. Qiu, D. Q.; Prentice P. Adv Polym Technol 1998, 17, 23.
16. Qu, J.; Columbo, P. Eur. Pat. 0,443,06B1 (1995).
17. Yanhong, F.; Jinping, Q. China Plast 2000, 14, 1.
18. Qu, J. Polym Plast Technol Eng 2002, 41, 115.